SLAC-PUB-1083
(ACC)
July 1972

FLUXOID QUANTIZATION AND PHASE TRANSITION IN HOLLOW SUPERCONDUCTORS CARRYING TRANSPORT CURRENT*

Mario Rabinowitz and Edward L. Garwin
Stanford Linear Accelerator Center
Stanford University, Stanford, California 94305

Abstract

A theory is presented to account for all the experimental observations of fluxoid quantization and phase transition in superconducting cylinders, without invoking the large, unlikely, misalignment between field and cylinder required in previous theory. Correct values are obtained for the ratio of periodic to background quadratic coefficients in the resistance vs. field plot, and for the 0° K penetration depth. The new theory predicts for the first time actual penetration depth and superconducting area.

From the earliest observation of periodicity in the transition temperature in units of the flux quantum h/2e by Little and Parks[1] (L-P) through to the most recent by Meyers and Meservey[2] (M-M), a quadratic background has been observed upon which the periodicity lies. Tinkham[3] derived an expression to explain the background seen by L-P. Yet, as he pointed out, unless their hollow cylinder were misaligned with the magnetic field, H, by as much as 9°, his theory differs by a factor of 100 from their result, and "a physical misalignment of this magnitude is unlikely, ...". P-L[4] observed "the nonperiodic quadratic background which appeared in all of the samples and which varied in magnitude depending upon the diameter of the cylindrical sample, the wall thickness, and the orientation of the sample in the magnetic field." Yet Tinkham's equation predicts no dependence on the cylinder diameter for an aligned cylinder.

On the other side of the coin, the recent experiments of M-M[2] show excellent agreement with Tinkham's theory. Therefore, the theory developed here will attempt to explain these two apparently disparate sets of results. Our effort here is in no way meant to lessen the value of Tinkham's basic analysis underlying the specifics of his theory, as we follow the same basic approach.

* Work supported by the U. S. Atomic Energy Commission.

(Submitted for publication)

Consider a thin superconducting cylindrical shell of length D, thickness d, and mean radius $R \gg d$, in an axial magnetic field $\vec{H}$. The penetration depth $\lambda > d$, so the field is approximately uniform across the wall. Since the wave function of the superconducting electrons is single-valued, we may apply the Bohr-Sommerfeld quantum condition to the electron pairs.

$$\oint \vec{P} \cdot \vec{d\ell} = q h, \tag{1}$$

where q is the quantum integer.

The canonical momentum, $\vec{P} = 2m\vec{v} + 2e\vec{A}$, where 2m is the mass, 2e is the charge, and v is the average center-of-mass velocity of the pairs. $\vec{A}$ is the magnetic vector potential so that the magnetic flux density $\vec{B} = \vec{\nabla} \times \vec{A} = \mu_0 \vec{H}$. Substituting into Eq. (1) and using Stokes's theorem, we have

$$\oint 2m\vec{v} \cdot d\vec{\ell} + \iint_S (\vec{\nabla} \times 2e\vec{A}) \cdot d\vec{S} = q h . \tag{2}$$

Equation (2) yields

$$v = \left(\frac{e}{2\pi m R}\right)\left(\frac{q h}{2e} - \pi R^2 B\right) . \tag{3}$$

The kinetic energy density associated with trapped flux quanta is

$$E = \frac{1}{2}\left(\frac{1}{2}n\right)(2m)v^2 = \frac{1}{2}nm\left(\frac{e}{2\pi m R}\right)^2\left(q\phi - \pi R^2 B\right)^2$$

$$= \frac{1}{2}\left(\frac{ne^2}{m}\right)\left(\frac{1}{2\pi R}\right)^2\left(q\phi - \pi R^2 B\right)^2 = \frac{1}{2\Lambda}\left(\frac{1}{2\pi R}\right)^2\left(q\phi - \pi R^2 B\right)^2 \tag{4}$$

where $\Lambda = m/ne^2 = \mu_0\lambda^2$, n is the number density of superconducting electrons, and $\phi = h/2e$ is the flux quantum for pairs.

As pointed out by Tinkham,[3] near T_c "due to inhomogeneity, one is dealing with isolated threads girdling the flux." However, he does not pursue this aspect of the theory near T_c in terms of the kinetic energy of the shielding currents of these filaments. It is likely that the regions of the grain boundaries become normal first, leaving superconducting regions of thickness d and average width w, each being a singly-connected surface with circulating current density J_c, as illustrated in Fig. 1. Parks and Little[4] pointed out that even with superconducting and normal regions, pairs can still traverse the cylinder circumference, and E is preserved. The London equation determines J_c,

$$\oint \Lambda \vec{J}_c \cdot \vec{d\ell} = -\iint_S \vec{B} \cdot \vec{dS} \ , \tag{5}$$

giving the approximate solution

$$J_c \doteq \frac{-1}{2\Lambda} \left(\frac{d\,w}{d + w}\right) B \ . \tag{6}$$

Since $J_c = \left(\frac{1}{2} n\right)(2e) v_c$, the shielding contribution to the kinetic energy density is

$$E_c = \frac{1}{2}\Lambda J_c^2 = \frac{1}{8\Lambda}\left(\frac{d\,w}{d + w}\right)^2 B^2 \ . \tag{7}$$

A transport current, I_p, parallel to the axis, is impressed on the cylinder (as is done experimentally to measure the resistance change of the cylinder as H is varied) by means of leads at each end. These electrons have total velocity, v_t, with a component of velocity v_s, due to H, around the cylinder in addition to the component of velocity v_p they have parallel to the cylinder's axis. The effect of the transport current has been neglected in the previous analyses.[1-6] Consider the power supply and normal leads to be equivalent to a superconducting wire attached to the ends of the cylinder in a plane parallel to $\vec{B}$. In this case, as before, Eq. (1) holds.[7]

Before proceeding, we point out that in all the experiments to date,[1,2,4,5] connection has been made to the cylinder by means of the thin film on the plate upon which the cylinder rests, i.e., at the bottom edge of the cylinder. Thus for small B, the spiralling electrons will not necessarily be collected in their first traversal of the cylinder, as they may reach the cylinder end at a point distant from the anode. In this case, we assume they will be specularly reflected at each end, and that for collection there are only discrete angles $\sigma = \mathrm{tn}^{-1} \frac{v_s}{v_p}$ as long as σ is small. Consideration that an electron must make an odd number of traversals for collection leads to the condition

$$\mathrm{tn}\,\sigma = \frac{2\pi R k}{D(2i+1)} , \tag{8}$$

where k and i = 1, 2, 3, ... k is the number of times the electron has gone around the cylinder, and 2i is the number of reflections. When $\mathrm{tn}\,\sigma$ is large, one may relax the capture condition, as tunnelling, space charge effects, and small perturbations allow collection with an essentially continuously variable $\mathrm{tn}\,\sigma = \frac{v_s}{v_p}$. For small σ (essentially small B for the experiments performed):

$$\oint \vec{P} \cdot d\vec{\ell} = \oint 2m\vec{v}_t \cdot d\vec{\ell} + \iint_S 2eB \cdot dS = qh . \tag{9}$$

$$\oint 2m\vec{v}_t \cdot d\vec{\ell} = 2m\left(v_s^2 + v_p^2\right)^{1/2} \left[(2i+1)^2 D^2 + (2\pi R k)^2\right]^{1/2} , \tag{10}$$

where the path of integration is chosen to lie deep within the connecting wire so that $v_t = 0$ there.

$$\iint_S 2e\vec{B} \cdot d\vec{S} = 2eBk\pi R^2 . \tag{11}$$

Combining Eq. (9), (10), and (11), we obtain the solution for the kinetic energy density associated with transport current, $E_{t1} = \frac{1}{2} n m \left(v_s^2 + v_p^2\right)$,

$$E_{t1} = (2\Lambda)^{-1}\left[(2i+1)^2 D^2 + (2\pi R k)^2\right]^{-1} (q\phi - k\pi R^2 B)^2 \quad , \tag{12}$$

for small σ (equivalently small B).

Now let us consider large σ (large B).

$$\oint 2m\vec{v}_t \cdot \vec{d\ell} = 2mv_t (2i+1) D\, (v_t/v_p) = 2m\left(v_s^2 + v_p^2\right)(2i+1)D/v_p \; . \tag{13}$$

$$\iint_S 2e\vec{B} \cdot \vec{dS} = eB(2i+1)DRv_s/v_p \tag{14}$$

Combining Eq. (9), (13), and (14), we find

$$v_s = \left\{-eRLB \pm \left[(eRLB)^2 - 8mLv_p(2mLv_p - qh)\right]^{1/2}\right\}/(4mL), \tag{15}$$

where $L = (2i+1)D$. Thus, in this case, the kinetic energy density is

$$E_{t2} = \frac{R^2B^2}{16\Lambda} + \frac{J_p}{2L}(q\phi - \Lambda L J_p) + \frac{1}{2}\left[\left(\frac{R^2B^2}{8\Lambda}\right)^2 + \frac{R^2B^2J_p}{4\Lambda L}(q\phi - \Lambda L J_p)\right]^{\frac{1}{2}} + \frac{1}{2}\Lambda J_p^2 \; , \tag{16}$$

where $J_p = nev_p = I_p/(2\pi R d)$.

Thus the total kinetic energy density of superconducting electrons in the cylinder is

$$E_{Tu} = E + E_c + E_{tu} \tag{17}$$

where $u = 1$ for small σ, and $u = 2$ for large σ.

For small σ, we have, on substituting the order parameter $\omega = \frac{\Lambda_0}{\Lambda}$,

$$E_{T1} = \left(2\Lambda_0\right)^{-1}(2\pi R)^{-2}(q\phi - \pi R^2 B)^2\omega + \left(8\Lambda_0\right)^{-1}\left(\frac{dw}{d+w}\right)^2 B^2\omega +$$

$$+ \left(2\Lambda_0\right)^{-1}\left[L^2 + (2\pi R k)^2\right]^{-1}(q\phi - k\pi R^2 B)^2\omega \; . \tag{18}$$

This must be added to the Ginzburg-Landau total free energy difference, thus

$$\Delta G(\omega, T) = -a(T)\,\omega + \frac{1}{2}\, b(T)\,\omega^2 + E_{T1}(\omega) \quad , \tag{19}$$

where the spatial variation of the order parameter $|\nabla\omega|^2$ is negligible due to the thinness of the cylinder.

$$a(T) = \mu_0 H(T)^2 \left[\lambda(T)/\lambda_0\right]^2 = \mu_0 H_0^2 (1-t^2)^2 (1-t^4)^{-1} = \mu_0 H_0^2 (1-t^2)(1+t^2)^{-1} \tag{20}$$

where H_0 is the thermodynamic critical field at 0° K, λ is the equilibrium penetration depth, and the reduced temperature $t = T/T_c$.

$$b(T) = a(T)\left[\lambda(T)/\lambda_0\right]^2 \quad . \tag{21}$$

We want $\frac{\partial \Delta G}{\partial \omega} = 0$ to find the minimum free energy difference, and set $\omega = 0$ for the transition condition of no superconducting electrons. Thus

$$0 = -\mu_0 H_0^2 (1-t^2)(1+t^2)^{-1} + \frac{\Lambda}{\Lambda_0}\, E + \frac{\Lambda}{\Lambda_0}\, E_c + \frac{\Lambda}{\Lambda_0}\, E_{t1} \, . \tag{22}$$

Expanding to first order in $\Delta t = \left[T_c - T_c(H)\right]/T_c \ll 1$, we have

$$\frac{T_c - T_c(H)}{T_c} = \frac{1}{8\lambda_0^2 \mu_0^2 H_0^2}\left[\frac{\left(q\phi - \pi R^2 B\right)^2}{\pi^2 R^2} + \left(\frac{d - w}{d + w}\right)^2 B^2 + \frac{4\left(q\phi - k\pi R^2 B\right)^2}{\left[L^2 + (2\pi R k)^2\right]}\right] \quad , \tag{23}$$

for small σ.

When k is small and/or L is large, Eq. (23) yields the results of M-M.[2] The other experimental results[1,4,5] also come naturally from Eq. (23) without the necessity of invoking misalignment. Let us look at the quadratic coefficients α_p and α_b, and include the possibility of a misalignment angle θ.

$$\text{Periodic parabola:} \quad (\Delta t)_{p,\,q=0} = \alpha_p B^2 = R^2 B^2 \cos^2\theta \left(8\lambda_0^2 \mu_0^2 H_0^2\right)^{-1} \, . \tag{24}$$

Background parabola:

$$(\Delta t)_b = \alpha_b B^2 = \left(8\lambda_0^2 \mu_0^2 H_0^2\right)^{-1} \left[\left(\frac{d\,w}{d+w}\right)^2 B^2 \cos^2\theta + \frac{4(\pi R^2)^2 \left(\frac{q}{x} - k\right)^2 B^2 \cos^2\theta}{\left[L^2 + (2\pi R k)^2\right]} + 4R^2 B^2 \sin^2\theta\right], \quad (25)$$

where for small θ and B the $\sin^2\theta$ misalignment term enters in as for Tinkham,[2] and $x = \pi R^2 B/\phi$. Therefore

$$\frac{\alpha_p}{\alpha_b} = R^2 \cos^2\theta \left[\left(\frac{d\,w}{d+w}\right)^2 \cos^2\theta + \frac{4(\pi R^2)^2 \left(\frac{q}{x} - k\right)^2 \cos^2\theta}{\left[L^2 + (2\pi R k)^2\right]} + 4R^2 \sin^2\theta\right]^{-1} . \quad (26)$$

Equation (26) is a simple quadratic in k, and can be solved exactly for k for all the different experimental values of α_p/α_b, with θ either $= 0$ or $\neq 0$ as the true case may be. The Sn data taken by L-P[1,4] is shown in Fig. 2 for reference.

Let us consider the L-P[1,4] data (a lower limit for $\frac{\alpha_p}{\alpha_b}$), and get an approximate solution for k which reveals the inherent simplicity between the parameters. In their data, $\frac{\alpha_p}{\alpha_b} \sim 10$ for Sn and ~ 25 for In. Hence $R^2 \gg \frac{\alpha_p}{\alpha_b}\left(\frac{d\,w}{d+w}\right)^2$. We may also neglect the $\sin^2\theta$ term if $R^2 \cos^2\theta \gtrsim 10\left(4\frac{\alpha_p}{\alpha_b} R^2 \sin^2\theta\right)$. Therefore, up to a 3° misalignment, the $\sin^2\theta$ term is negligible. Also for $x \geq 1$, $k \gg \frac{q}{x} \sim 1$. With these approximations, Eq. (26) reduces to

$$k \doteq (2i+1)\,D\,(2\pi R)^{-1}\left(\frac{\alpha_p}{\alpha_b} - 1\right)^{-1/2} \qquad \text{(for L-P)} \quad (27)$$

The upper limit of $\frac{\alpha_p}{\alpha_b}$ comes from the M-M[2] data in which $\theta = 0$, and $\alpha_p/\alpha_b \doteq 3R^2/d^2$ so that $(\alpha_p/\alpha_b)\left(\frac{d\,w}{d+w}\right)^2 = \frac{3}{N}R^2$, where $N = d^2\left(\frac{d+w}{d\,w}\right)^2$, e.g., N=4 when w = d. Equation (26) gives

$$k \doteq (2i+1)\,D\,(2\pi R)^{-1}\left[\frac{N}{N-3}\left(\frac{\alpha_p}{\alpha_b} - 1\right)\right]^{-1/2} \qquad (\text{for M-M, } x \geq 1). \quad (28)$$

Thus with the values of k from Eq. (27) or (28), one may obtain values of λ_0 and α_p/α_b consistent with all the experiments, without invoking misalignment.

Furthermore, values of $\lambda(T)$ and T may be obtained from this theory and the experimental data, which cannot be obtained from Tinkham's theory.[2]

From Eq. (8), we have

$$J_p = m v_s (2i+1) D \left(\mu_0 \lambda^2 e 2\pi R k\right)^{-1} . \tag{29}$$

Substituting for v_s from Eq. (12), and solving for λ,

$$\lambda(T) = \left(\phi/\mu_0 J_p\right)^{1/2} (kx-q)^{1/2} \left[(2i+1)^2 D^2 + 2(2\pi R k)^2 + \frac{(2\pi R k)^4}{(2i+1)^2 D^2}\right]^{-1/4} . \tag{30}$$

Equations (27) and (28) in (30) yield

$$\lambda(T) \doteq \left(\phi x/2\pi R \mu_0 J_p\right)^{1/2} \left[\frac{\alpha_p}{\alpha_b} + 1\right]^{-1/4} \qquad \text{(for L-P), and} \tag{31}$$

$$\lambda(T) \doteq \left(\phi x/2\pi R \mu_0 J_p\right)^{1/2} \left[\left(\frac{N}{N-3}\right) \frac{\alpha_p}{\alpha_b}\right]^{-1/4} \qquad \text{(for M-M)} . \tag{32}$$

Now $\lambda(T) = \lambda_0 (1-t^4)^{-1/2} \doteq \frac{1}{2} \lambda_0 (1-t)^{-1/2}$ for $t \doteq 1$. (This appears to fit the experimental data as well or better than the BCS expression.) Therefore

$$T \doteq T_c \left[1 - \frac{1}{4} (\lambda_0/\lambda)^2\right] . \tag{33}$$

Values of λ from Eq. (31) and (32), when substituted into (33), give values of T which agree well with experiment.[1,2,4] Since the cylindrical shell may break up into superconducting and normal regions, J_p may be $> I_p/2\pi R d$. When T is given, then from Eq. (31), (32), and (33), one may calculate the true J_p and hence the effective cross sectional area which remains superconducting.

It should now be clear that the transport current, I_p, plays a vital role in the experimental results, though it was totally neglected in the previous analyses,[1-6] having been regarded merely as a means for sensing the phase transition. I_p causes a spiralling electron trajectory, a change in the path length of which affects v_s and hence the quadratic background. For a given flux, the number of quantum mechanical wavelengths is conserved, but the electron total path length is a function of I_p, and therefore so is the electron wavelength, with a concomitant inverse change in electron momentum.

References

1. W. A. Little and R. D. Parks, Phys. Rev. Letters 9, 9 (1962).
2. L. Meyers and R. Meservey, Phys. Rev. B 4, 824 (1971).
3. M. Tinkham, Phys. Rev. 129, 2413 (1963).
4. R. D. Parks and W. A. Little, Phys. Rev. 133, A97 (1964).
5. R. P. Groff and R. D. Parks, Phys. Rev. 176, 567 (1968).
6. D. H. Douglas, Jr., Phys. Rev. 132, 513 (1963).
7. If only the London Eq. (5) applies, this is equivalent to a 0 angular momentum state with $q = 0$.

Figure captions

Fig. 1. Thin-walled superconducting cylindrical shell showing shielding current density J_c.

Fig. 2. Variation of resistance of tin cylinder with magnetic field at its transition temperature showing a periodic parabolic array superimposed upon a quadratic background (from L-P[1,4]).

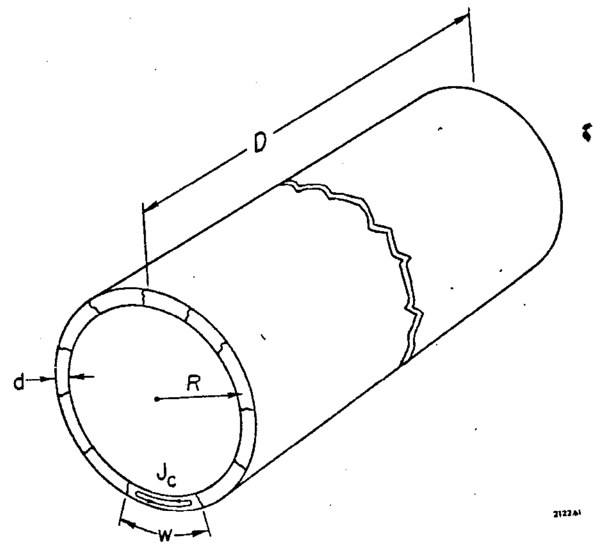

FIG. 1

TOP

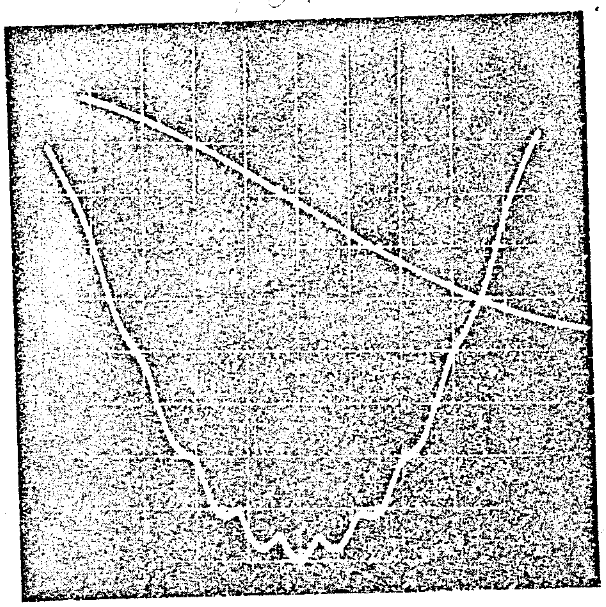

FIG. 2